Acta Crystallographica Section C
Structural Chemistry
ISSN 2053-2296

A candidate for a single-chain magnet: $[Mn_3(OAc)_6(py)_2(H_2O)_2]_n$ (OAc is acetate and py is pyridine)

Judith Caballero-Jiménez,[a] Yasmi Reyes Ortega,[a]* Sylvain Bernès[b]‡ and Roberto Escudero[c]

[a]Centro de Química, Instituto de Ciencias, Universidad Autónoma de Puebla, Edif. 194 Complejo de Ciencias CU, San Manuel, 72570 Puebla, Pue., Mexico, [b]DEP Facultad de Ciencias Químicas, UANL, Guerrero y Progreso S/N, Col. Treviño, 64570 Monterrey, NL, Mexico, and [c]Instituto de Investigaciones en Materiales, UNAM, Circuito Exterior, Ciudad Universitaria, Coyoacan, 04510 México DF, Mexico
Correspondence e-mail: yasmi.reyes@correo.buap.mx

Received 11 April 2014
Accepted 26 June 2014

The title complex, *catena*-poly[di-μ_3-acetato-$\kappa^6O:O:O'$-tetra-μ_2-acetato-$\kappa^4O:O;\kappa^4O:O'$-diaquabis(pyridine-κN)trimanganese(II)], $[Mn_3(CH_3COO)_6(C_6H_5N)_2(H_2O)_2]_n$, is a true one-dimensional coordination polymer, in which the Mn^{II} centres form a zigzag chain along [010]. The asymmetric unit contains two metal centres, one of which (Mn1) lies on an inversion centre, while the other (Mn2) is placed close to an inversion centre on a general position. Since all the acetates behave as bridging ligands, although with different μ_2- and μ_3-coordination modes, a one-dimensional polymeric structure is formed, based on trinuclear repeat units (Mn1···Mn2···Mn2′), in which the Mn2 and Mn2′ sites are related by an inversion centre. Within this monomeric block, the metal–metal separations are Mn1···Mn2 = 3.36180 (18) Å and Mn2···Mn2′ = 4.4804 (3) Å. Cation Mn1, located on an inversion centre, displays an $[MnO_6]$ coordination sphere, while Mn2, on a general position, has a slightly stronger $[MnO_5N]$ ligand field, as the sixth coordination site is occupied by a pyridine molecule. Both centres approximate an octahedral ligand field. The chains are parallel in the crystal structure and interact *via* hydrogen bonds involving coordinated water molecules. However, the shortest metal–metal separation between two chains [5.3752 (3) Å] is large compared with the intrachain interactions. These structural features are compatible with a single-chain magnet behaviour, as confirmed by preliminary magnetic studies.

Keywords: crystal structure; manganese carboxylate cluster; one-dimensional polymer; qubit-based computation materials; single-molecule magnet; single-chain magnets; Ising one-dimensional system.

‡ Currently unaffiliated to UANL.

1. Introduction

Manganese carboxylate cluster chemistry is now widely recognized as a field from which materials suitable for qubit-based computation could emerge. That chemistry was pioneered by George Christou and David Hendrickson, among others, with the fruitful Mn_{12} line of compounds, including the emblematic cluster $[Mn_{12}O_{12}(O_2CPh)_{16}(H_2O)_4]$ (Boyd *et al.*, 1988; Sessoli *et al.*, 1993). This mixed-valence cluster displays the two essential features required for a single-molecule magnet (SMM), *i.e.* a high-spin ground state and a large negative magnetic anisotropy. However, the most impressive behaviour reported for these clusters is the resonant quantum tunnelling of magnetization, which is a key property for molecular spintronics (Perenboom *et al.*, 1998; Hill *et al.*, 2003, 2010). Like SMM clusters, some chain-shaped molecules also exhibit bistability and slow relaxation of their magnetization. These compounds, termed single-chain magnets (SCM), have their magnetic behaviour affected not only by the magnetic anisotropy of the spins but also by their intrachain magnetic interactions (Coronado *et al.*, 2003; Brooker & Kitchen, 2009; Zhang *et al.*, 2013).

Although many synthetic approaches have been described in the literature, the rational design of a synthesis for a given manganese carboxylate cluster is hindered by the fine tuning of the following parameters: the oxidation states of the metal centres; the suitability of the symmetry of the ligand field for the 3*d* orbitals centred on the metals; the coordination modes of the carboxylate ligands; and competition with ancillary ligands. Moreover, both the nuclearity and dimensionality of the resulting structure are quite unpredictable, with a large range of possibilities, from isolated SMMs, which may be described as zero-dimensional nanoparticles, to three-dimensional polymeric architectures, which may be considered as bulk materials.

While working on the synthesis of such compounds, we obtained a one-dimensional coordination polymer, namely $[Mn_3(OAc)_6(py)_2(H_2O)_2]_n$ (OAc is acetate and py is pyridine), (I), which is a candidate for a new SCM.

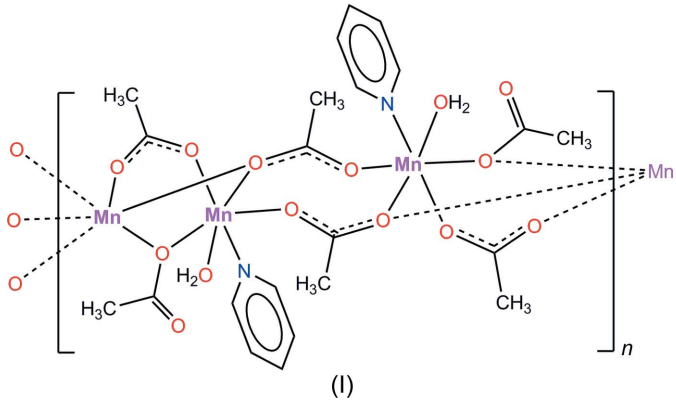

(I)

2. Experimental

2.1. Synthesis, crystallization and SQUID magnetometry

All synthetic and post-synthetic work was carried out under aerobic conditions. The reagents and solvents were obtained

  doi:10.1107/S2053229614015137

Table 1
Experimental details.

Crystal data	
Chemical formula	$[Mn_3(C_2H_3O_2)_6(C_6H_5N)_2(H_2O)_2]$
M_r	713.31
Crystal system, space group	Triclinic, $P\overline{1}$
Temperature (K)	200
a, b, c (Å)	8.1153 (2), 9.0404 (2), 10.0759 (2)
α, β, γ (°)	83.160 (1), 81.994 (1), 77.423 (1)
V (Å^3)	711.43 (3)
Z	1
Radiation type	Mo $K\alpha$
μ (mm^{-1})	1.38
Crystal size (mm)	0.15 × 0.12 × 0.12
Data collection	
Diffractometer	Bruker APEXII CCD area-detector diffractometer
Absorption correction	Multi-scan (*SADABS*; Bruker, 2009)
T_{min}, T_{max}	0.820, 0.852
No. of measured, independent and observed [$I > 2\sigma(I)$] reflections	11780, 3514, 3269
R_{int}	0.012
(sin $\theta/\lambda)_{max}$ (Å^{-1})	0.667
Refinement	
$R[F^2 > 2\sigma(F^2)]$, $wR(F^2)$, S	0.020, 0.057, 1.06
No. of reflections	3514
No. of parameters	198
H-atom treatment	H atoms treated by a mixture of independent and constrained refinement
$\Delta\rho_{max}$, $\Delta\rho_{min}$ (e Å^{-3})	0.31, −0.35

Computer programs: *APEX2* (Bruker, 2009), *XPREP* (Bruker, 2009), *SHELXS2013* (Sheldrick, 2008), *SHELXL2013* (Sheldrick, 2008), *SHELXTL* (Sheldrick, 2008) and *Mercury* (Macrae *et al.*, 2008).

from commercial sources and used without further purification. IR analyses were performed using a Nicolet Nexus 6700 FT–IR spectrometer in the 4000–600 cm^{-1} range. Compound (I) was prepared by the addition of excess pyridine (12.41 mmol, 1 ml) to a hot solution of $Mn(OAc)_2{\cdot}4H_2O$ (1 mmol, 0.245 g) in EtOH (95%; 5 ml). The solution was stirred for 30 min and filtered, and then layered with Et_2O. After 1 d, colourless crystals of (I) were obtained from this solution by slow diffusion of Et_2O (yield 48%). IR (KBr pellet, ν_{max}, cm^{-1}): 3252 (*br*), 2943 (*s*), 2878 (*s*), 1557 (*m*), 1414 (*m*), 1004 (*st*), 877 (*m*), 658 (*m*), 606 (*m*). Magnetic susceptibility measurements on powdered crystals were carried out using a Quantum Design SQUID magnetometer at 2 K under an applied field H of −50000 to 50000 Oe, and in the temperature range 2–300 K at H = 1000 Oe. Correction for the diamagnetic contribution of the constituent atoms was applied using Pascal's constants.

2.2. Refinement

Crystal data, data collection and structure refinement details are summarized in Table 1. The collection of diffraction data (work done in Canada) and the final structure refinement (work done in Mexico) were routine. All C-bound H atoms were placed in calculated positions, with C—H = 0.95 (pyridine) or 0.98 Å (methyl). Methyl groups were considered as rigid tetrahedral groups free to rotate about their C—C bonds. Isotropic displacement parameters for these H atoms were calculated as U_{iso}(H) = 1.2U_{eq}(C) for the pyridine molecule and 1.5U_{eq}(C) for the methyl groups. Atoms H71 and H72 of the water molecule were clearly detected in a difference map and were refined with free coordinates and isotropic displacement parameters.

3. Results and discussion

Although the synthesis of (I) was carried out under aerobic conditions, the complex is an Mn^{II} species with the formula $[Mn_3(OAc)_6(H_2O)_2(py)_2]_n$, where OAc and py are acetate and pyridine ligands, respectively. One manganese ion, Mn1, is located on an inversion centre in the triclinic unit cell, and the other, Mn2, is located on a general position, close to an inversion centre. Three acetate ligands are bonded to Mn1, using three coordination modes (Fig. 1). The first acetate (atoms O1/O2) bridges independent Mn centres in the common 2.11 *syn–syn* mode [for Harris coordination nomenclature, see Coxall *et al.* (2000)], found, for example, in the starting material manganese diacetate, $Mn(OAc)_2{\cdot}4H_2O$ (Bertaut *et al.*, 1974; Nicolaï *et al.*, 2001), and also in $Co(OAc)_2{\cdot}H_2O$ (Zhang *et al.*, 2010) and other simple divalent metal salts. Acetate O5/O6 bridges the same metal centres Mn1 and Mn2 in the 2.20 coordination mode, which is much less frequently observed. For Mn-based coordination polymers, only two cases have been reported to date in which this coordination mode for acetate is found, *viz.* $[Mn_3(OAc)_6(H_2O)_4]{\cdot}2H_2O$ (Cheng & Wang, 1991) and a complex polymer with a chain-like structure (Xu *et al.*, 2009). Finally, the polymeric nature of (I) is fixed by the third acetate, O3/O4, in the 3.12 coordination mode, between Mn1 and Mn2 in the asymmetric unit and a symmetry-related Mn2^i site [symmetry code: (i) $-x+1, -y+1, -z+1$]. This arrangement for polymerization is identical to that found in $Mn(OAc)_2{\cdot}4H_2O$

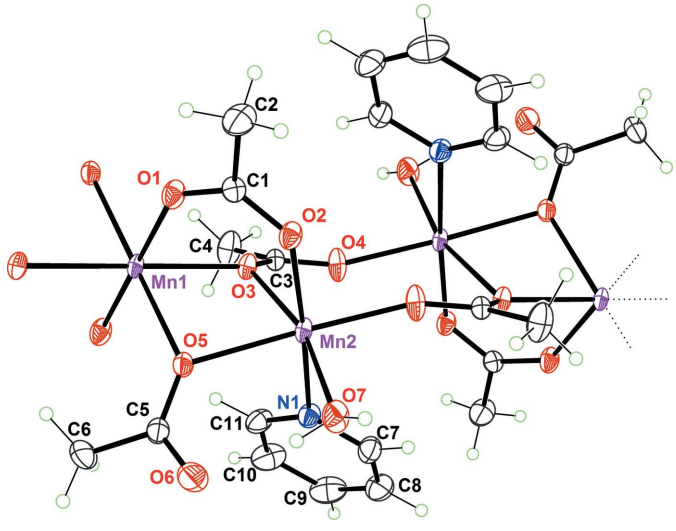

Figure 1
Part of the polymeric chain of (I), limited to two Mn1···Mn2 units related by an inversion centre. Coordination spheres for the Mn1···Mn2···Mn2^i monomer are complete, and the asymmetric unit is labelled. Nonlabelled atoms are generated by the symmetry operator ($-x+1, -y+1, -z+1$). Displacement ellipsoids are drawn at the 50% probability level.

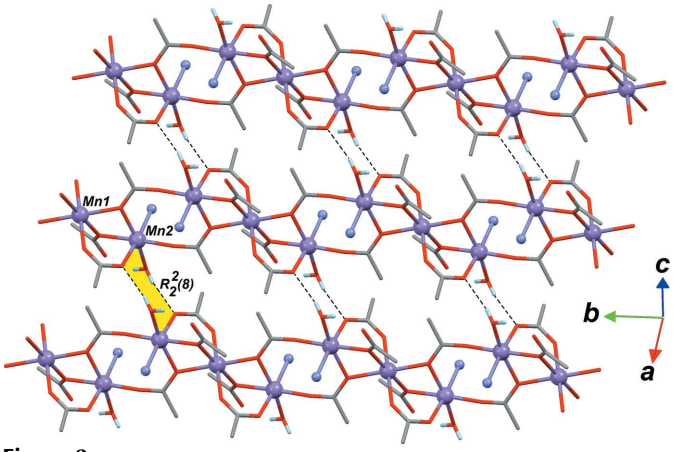

Figure 2
Part of the crystal structure of (I), showing three chains in the [010] direction and the $R_2^2(8)$ rings connecting the chains (dashed bonds). For the sake of clarity, pyridine ligands bonded to Mn2 centres are drawn with a single N atom (blue spheres), and all methyl H atoms have been omitted.

(Bertaut *et al.*, 1974) and α-Mn(OAc)$_2$ (Lin *et al.*, 2009), and in more complex polymeric compounds with various dimensionalities (*e.g.* Zartilas *et al.*, 2008; Weng *et al.*, 2008; Wan *et al.*, 2010). These different μ_2- and μ_3-bridging modes are reflected in the IR spectrum (see *Supporting information*) of (I): the ν_{asym} and ν_{sym} vibration modes for the COO$^-$ groups are split into two or three bands around 1557 and 1414 cm^{-1}, respectively.

The arrangement of the acetate ligands completes the octahedral coordination environment for the centrosymmetric Mn1 centre. This metal centre presents an [MnO$_6$] ligand field with the symmetry lowered from octahedral to C_i, because the Mn1—O bond lengths for each acetate are significantly different: Mn1—O1 = 2.1369 (9) Å, Mn1—O3 = 2.1997 (8) Å and Mn1—O5 = 2.2277 (8) Å. The coordination environment for Mn2, which is in a general position, is completed with neutral ligands, H$_2$O and pyridine, present in the reaction media. Mn2 thus has an [MnO$_5$N] coordination, with a ligand field probably slightly stronger than that for Mn1 and a large deviation from octahedral symmetry: the coordination bond lengths for Mn2 are in the range 2.0995 (9)–2.2946 (10) Å and the *trans* angles are in the range 164.84 (4)–176.87 (4)°.

The one-dimensional polymeric chain of (I), formed *via* inversion centres, runs in the [010] direction (Fig. 2). Within the asymmetric unit, the Mn1···Mn2 separation is 3.36180 (18) Å and the Mn2···Mn2^i distance, allowing polymerization, is longer, at 4.4804 (3) Å. Both distances are unexceptional, considering that, in Mn–acetate-based polymers, they span a large range, *ca* 2.5–5.2 Å (Allen, 2002), allowing a variety of magnetic ground states for these materials. In the present case, the long metal–metal separations alternate along the chain with the dimers possessing the short separation. Parallel chains are packed in the crystal structure, and the cohesion is maintained through O—H···O hydrogen bonds of moderate strength, using the coordinated water molecules as donors (Fig. 2 and Table 2). The graph set (Bernstein *et al.*, 1995) resulting from two inversion-related

Table 2
Hydrogen-bond geometry (Å, °).

D—H···A	D—H	H···A	D···A	D—H···A
O7—H71···O6	0.81 (2)	1.92 (2)	2.6694 (15)	154 (2)
O7—H72···O2^i	0.78 (2)	2.05 (2)	2.8162 (13)	169 (2)

Symmetry code: (i) $-x+2, -y+1, -z+1$.

interchain hydrogen bonds is $R_2^2(8)$, common in water–acetate systems. The metal–metal distance in the $R_2^2(8)$ ring is Mn2···Mn2^{ii} = 5.3752 (3) Å [symmetry code: (ii) $-x+2, -y+1, -z+1$]. Since this distance is much longer than the metal–metal distances along the chain, (I) should be considered as a true one-dimensional coordination polymer, rather than a two-dimensional material. In spite of its low dimensionality, this material is a densely packed system, reaching a high Kitaigorodski packing coefficient of C_K = 0.733 (*PLATON*; Spek, 2009).

The above-described geometric features are encouraging and make (I) a candidate for being an Ising one-dimensional system (Sun *et al.*, 2010) behaving as a ferri- or ferromagnet. Assuming a weak enough crystal-field splitting, high-spin d^5 electronic configurations may be expected for the Mn^{II} centres. The anisotropic trinuclear units (Mn1···Mn2···Mn2^i) have distances between the magnetic sites that are suitable for ferromagnetic interactions. Indeed, these distances, of 3.36 and 4.48 Å, may be compared with those observed in the first heterometallic Mn^{III}–Ni^{II} polymeric SCM synthesized in 2002: Mn^{III}···Mn^{III} = 3.42 Å and Mn^{III}···Ni^{II} = 5.06 Å (Clérac *et al.*, 2002). Thus, the actual nature of the magnetic behaviour for the title Mn^{II} polymer should be defined mainly by interchain contacts resulting from the $R_2^2(8)$ ring motifs. A search of the Cambridge Structural Database (Version 5.35, updated May 2014; Allen, 2002) retrieved 139 similar $R_2^2(8)$ rings in Mn compounds, with coordinated water molecules as donors and carboxylate O atoms as acceptors. Most of them are associated with first-level centrosymmetric patterns $\mathbf{R}(\vec{a}\vec{a})$, as in (I), and the others belong to second-level patterns $\mathbf{R}(\vec{a}\vec{b})$ according to Motherwell's graph-set nomenclature (Motherwell *et al.*, 2000). The important feature to be considered, bearing the magnetic properties in mind, is the poor flexibility of this ring: for $\mathbf{R}(\vec{a}\vec{a})$ patterns, the ring has a chair conformation and the metal–metal interaction is determined mainly by the puckering parameters, while $\mathbf{R}(\vec{a}\vec{b})$ patterns may adopt a folded conformation, allowing shorter metal–metal interactions. In the subset of 139 hits, regardless of the Mn oxidation state and the dimensionality of the crystal structure, the Mn···Mn separation in $R_2^2(8)$ rings is in the range 4.77–6.32 Å. Interestingly, the shortest separation was reported for a complex Mn$_{22}$ cluster, in which the $R_2^2(8)$ ring links two molecules. This mixed-valence compound is an SMM with quantum tunnelling of magnetization (Brockman *et al.*, 2007). Thus, it may be inferred that the $R_2^2(8)$ ring in (I) is not an efficient exchange pathway, making a strong antiferromagnetic interchain coupling unlikely.

Preliminary magnetic measurements of (I) are in agreement with this structural description. At room temperature, the title

complex shows a $\chi_m T$ value of 13.15 $cm^3\ mol^{-1}$ K, which is very close to that calculated for three non-interacting $S_i = \frac{5}{2}$ centres, 13.12 $cm^3\ mol^{-1}$ K, assuming a spin-only model (g_{Mn} = 2.00; Christian *et al.*, 2004). A plot of *M versus T* shows different magnetization pathways below a critical temperature T_C = 50 K, pointing to superparamagnetic behaviour. On the other hand, a hysteresis loop in the *M*(*H*) plot is observed (Fig. 3), indicative of ferromagnetic exchange interactions (Bertotti, 1998). Experimentally, an SCM shows both superparamagnet-like properties with frequency-dependent out-of-phase signals in AC susceptibility measurements, and hysteresis in *M versus* applied DC field measurements (King *et al.*, 2004; Brockman *et al.*, 2007). Therefore, AC magnetic susceptibility measurements are currently being carried out, in order to characterize further the potential SCM behaviour of this new polymer.

The authors thank CONACyT Mexico (project No. BUAP-CA-261) and the Autonomous University of Puebla (project Nos. Y-NAT-12-I and Y-NAT-13-I) for financial support, and Dr Ilia Korobkov (University of Ottawa) for assistance in the collection of the diffraction data. RE thanks DGAPA–UNAM (project No. IN106014), CONACyT (project No. 129293, Ciencia Básica), BISNANO, and project No. PICCO 11-7 supported by the Institute of Sciences of Distrito Federal, Mexico City.

Supporting information for this paper is available from the IUCr electronic archives (Reference: YP3067).

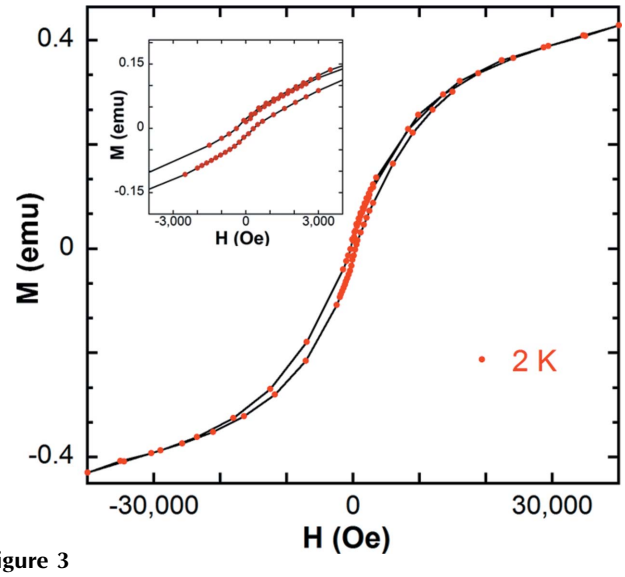

Figure 3
Magnetization (*M*) *versus* applied magnetic field (*H*) hysteresis loop for (I) at *T* = 2 K. The inset focuses on the experimental data in the −3000 to 3000 Oe range.

References

Allen, F. H. (2002). *Acta Cryst.* B**58**, 380–388.
Bernstein, J., Davis, R. E., Shimoni, L. & Chang, N.-L. (1995). *Angew. Chem. Int. Ed. Engl.* **34**, 1555–1573.
Bertaut, E. F., Tran Qui, D., Burlet, P., Burlet, P., Thomas, M. & Moreau, J. M. (1974). *Acta Cryst.* B**30**, 2234–2236.
Bertotti, G. (1998). *Hysteresis in Magnetism*, 1st ed., edited by G. Bertotti. San Diego: Academic Press.
Boyd, P. D. W., Li, Q., Vincent, J. B., Folting, K., Chang, H. R., Streib, W. E., Huffman, J. C., Christou, G. & Hendrickson, D. N. (1988). *J. Am. Chem. Soc.* **110**, 8537–8539.
Brockman, J. T., Stamatatos, T. C., Wernsdorfer, W., Abboud, K. A. & Christou, G. (2007). *Inorg. Chem.* **46**, 9160–9171.
Brooker, S. & Kitchen, J. A. (2009). *Dalton Trans.* pp. 7331–7340.
Bruker (2009). *APEX2*, *XPREP* and *SADABS*, Bruker AXS Inc., Madison, Wisconsin, USA.
Cheng, C.-Y. & Wang, S.-L. (1991). *Acta Cryst.* C**47**, 1734–1736.
Christian, P., Rajaraman, G., Harrison, A., Helliwell, M., McDouall, J. J. W., Raftery, J. & Winpenny, R. E. P. (2004). *Dalton Trans.* pp. 2550–2555.
Clérac, R., Miyasaka, H., Yamashita, M. & Coulon, C. (2002). *J. Am. Chem. Soc.* **124**, 12837–12844.
Coronado, E., Palacio, F. & Veciana, J. (2003). *Angew. Chem. Int. Ed.* **42**, 2570–2572.
Coxall, R. A., Harris, S. G., Henderson, D. K., Parsons, S., Tasker, P. A. & Winpenny, R. E. P. (2000). *J. Chem. Soc. Dalton Trans.* pp. 2349–2356.
Hill, S., Datta, S., Liu, J., Inglis, R., Milios, C. J., Feng, P. L., Henderson, J. J., del Barco, E., Brechin, E. K. & Hendrickson, D. N. (2010). *Dalton Trans.* pp. 4693–4707.
Hill, S., Edwards, R. S., Jones, S. I., Dalal, N. S. & North, J. M. (2003). *Phys. Rev. Lett.* **90**, 217204.
King, P., Wernsdorfer, W., Abboud, K. A. & Christou, G. (2004). *Inorg. Chem.* **43**, 7315–7323.
Lin, J., Yuan, L., Guo, D.-W., Zhang, G., Yao, S.-Y. & Tian, Y.-Q. (2009). *Struct. Chem.* **20**, 505–508.
Macrae, C. F., Bruno, I. J., Chisholm, J. A., Edgington, P. R., McCabe, P., Pidcock, E., Rodriguez-Monge, L., Taylor, R., van de Streek, J. & Wood, P. A. (2008). *J. Appl. Cryst.* **41**, 466–470.
Motherwell, W. D. S., Shields, G. P. & Allen, F. H. (2000). *Acta Cryst.* B**56**, 466–473.
Nicolaï, B., Kearley, G. J., Cousson, A., Paulus, W., Fillaux, F., Gentner, F., Schröder, L. & Watkin, D. (2001). *Acta Cryst.* B**57**, 36–44.
Perenboom, J. A. A. J., Brooks, J. S., Hill, S. O., Hathaway, T. & Dalal, N. S. (1998). *Physica B*, **246–247**, 294–298.
Sessoli, R., Tsai, H. L., Schake, A. R., Wang, S., Vincent, J. B., Folting, K., Gatteschi, D., Christou, G. & Hendrickson, D. N. (1993). *J. Am. Chem. Soc.* **115**, 1804–1816.
Sheldrick, G. M. (2008). *Acta Cryst.* A**64**, 112–122.
Spek, A. L. (2009). *Acta Cryst.* D**65**, 148–155.
Sun, H.-L., Wang, Z.-M. & Gao, S. (2010). *Coord. Chem. Rev.* **254**, 1081–1100.
Wan, C.-Q., Xiao, N.-Y. & Wang, Z.-J. (2010). *Acta Cryst.* E**66**, m1478.
Weng, Z.-H., Chen, Z.-L. & Liang, F.-P. (2008). *Acta Cryst.* C**64**, m64–m66.
Xu, X.-X., Liu, X.-X., Zhang, X. & Sun, T. (2009). *Transition Met. Chem.* **34**, 827–833.
Zartilas, S., Moushi, E. E., Nastopoulos, V., Boudalis, A. K. & Tasiopoulos, A. J. (2008). *Inorg. Chim. Acta*, **361**, 4100–4106.
Zhang, W.-X., Ishikawa, R., Breedlove, B. & Yamashita, M. (2013). *RSC Adv.* **3**, 3772–3798.
Zhang, G., Lin, J., Guo, D.-W., Yao, S.-Y. & Tian, Y.-Q. (2010). *Z. Anorg. Allg. Chem.* **636**, 1401–1404.

supporting information

Acta Cryst. (2014). C**70**, 754-757 [doi:10.1107/S2053229614015137]

A candidate for a single-chain magnet: $[Mn_3(OAc)_6(py)_2(H_2O)_2]_n$ (OAc is acetate and py is pyridine)

Judith Caballero-Jiménez, Yasmi Reyes Ortega, Sylvain Bernès and Roberto Escudero

Computing details

Data collection: *APEX2* (Bruker, 2009); cell refinement: *APEX2* (Bruker, 2009); data reduction: *XPREP* (Bruker, 2009); program(s) used to solve structure: *SHELXS2013* (Sheldrick, 2008); program(s) used to refine structure: *SHELXL2013* (Sheldrick, 2008); molecular graphics: *SHELXTL* (Sheldrick, 2008) and *Mercury* (Macrae *et al.*, 2008); software used to prepare material for publication: *SHELXL2013* (Sheldrick, 2008).

***catena*-Poly[di-μ_3-acetato-$\kappa^6O:O:O'$-tetra-μ_2-acetato-$\kappa^4O:O;\kappa^4O:O'$-diaquabis(pyridine-κN)trimanganese(II)]**

Crystal data

$[Mn_3(C_2H_3O_2)_6(C_6H_5N)_2(H_2O)_2]$
M_r = 713.31
Triclinic, $P\overline{1}$
a = 8.1153 (2) Å
b = 9.0404 (2) Å
c = 10.0759 (2) Å
α = 83.160 (1)°
β = 81.994 (1)°
γ = 77.423 (1)°
V = 711.43 (3) Å^3
Z = 1
$F(000)$ = 365
D_x = 1.665 Mg m^{-3}
Melting point: 493 K
Mo $K\alpha$ radiation, λ = 0.71073 Å
Cell parameters from 9432 reflections
θ = 2.3–28.3°
μ = 1.38 mm^{-1}
T = 200 K
Block, colourless
0.15 × 0.12 × 0.12 mm

Data collection

Bruker APEXII CCD area-detector diffractometer
Radiation source: fine-focus sealed tube
Graphite monochromator
φ and ω scans
Absorption correction: multi-scan (*SADABS*; Bruker, 2009)
T_{min} = 0.820, T_{max} = 0.852
11780 measured reflections
3514 independent reflections
3269 reflections with $I > 2\sigma(I)$
R_{int} = 0.012
θ_{max} = 28.3°, θ_{min} = 2.3°
h = −10→10
k = −12→12
l = −13→13

Refinement

Refinement on F^2
Least-squares matrix: full
$R[F^2 > 2\sigma(F^2)]$ = 0.020
$wR(F^2)$ = 0.057
S = 1.06
3514 reflections
198 parameters
0 restraints
0 constraints
Primary atom site location: structure-invariant direct methods
Secondary atom site location: difference Fourier map
Hydrogen site location: inferred from neighbouring sites

H atoms treated by a mixture of independent and constrained refinement
$w = 1/[\sigma^2(F_o^2) + (0.031P)^2 + 0.2663P]$ where $P = (F_o^2 + 2F_c^2)/3$

$(\Delta/\sigma)_{max} = 0.001$
$\Delta\rho_{max} = 0.31$ e Å^{-3}
$\Delta\rho_{min} = -0.35$ e Å^{-3}

Special details

Experimental. Data collection was performed with four batch runs at phi = 0.00° (600 frames), at phi = 90.00° (600 frames), at phi = 180.00° (600 frames) and at phi = 270.00° (600 frames). A fifth batch run was collected at phi = 0.00° (50 frames) to monitor crystal and diffractometer stability. Frame width = 0.30° in omega. Data were merged, corrected for decay (if any), and treated with multi-scan absorption corrections (if required).

Fractional atomic coordinates and isotropic or equivalent isotropic displacement parameters (Å²)

	x	*y*	*z*	U_{iso}*/U_{eq}
Mn1	0.5000	1.0000	0.5000	0.01484 (6)
Mn2	0.67310 (2)	0.63019 (2)	0.56849 (2)	0.01492 (6)
N1	0.49468 (13)	0.58131 (12)	0.75859 (11)	0.0203 (2)
O1	0.69813 (11)	0.93862 (10)	0.34097 (9)	0.02220 (18)
O2	0.81744 (11)	0.69304 (9)	0.38176 (9)	0.02006 (17)
O3	0.43984 (10)	0.77516 (9)	0.49460 (9)	0.01721 (16)
O4	0.30799 (13)	0.58516 (10)	0.49762 (11)	0.0290 (2)
O5	0.66602 (11)	0.85585 (9)	0.64449 (9)	0.01837 (17)
O6	0.83746 (14)	0.78614 (12)	0.80527 (11)	0.0335 (2)
O7	0.89280 (13)	0.53570 (12)	0.67585 (11)	0.0269 (2)
H71	0.908 (3)	0.601 (3)	0.718 (2)	0.046 (6)*
H72	0.980 (3)	0.482 (2)	0.659 (2)	0.041 (5)*
C1	0.80320 (14)	0.81979 (13)	0.31196 (12)	0.0176 (2)
C2	0.92106 (19)	0.83031 (17)	0.18292 (15)	0.0327 (3)
H2A	1.0210	0.7471	0.1864	0.049*
H2B	0.9572	0.9281	0.1719	0.049*
H2C	0.8615	0.8225	0.1066	0.049*
C3	0.30526 (14)	0.72234 (13)	0.49728 (11)	0.0164 (2)
C4	0.13774 (16)	0.83251 (15)	0.50462 (17)	0.0306 (3)
H4A	0.0509	0.7845	0.4793	0.046*
H4B	0.1475	0.9232	0.4427	0.046*
H4C	0.1053	0.8619	0.5967	0.046*
C5	0.72135 (15)	0.87587 (13)	0.75330 (12)	0.0192 (2)
C6	0.6347 (2)	1.01701 (16)	0.82145 (15)	0.0323 (3)
H6A	0.7028	1.0322	0.8898	0.048*
H6B	0.5218	1.0051	0.8644	0.048*
H6C	0.6232	1.1054	0.7544	0.048*
C7	0.50630 (18)	0.43829 (15)	0.81537 (14)	0.0264 (3)
H7A	0.6018	0.3634	0.7860	0.032*
C8	0.3863 (2)	0.39423 (17)	0.91456 (15)	0.0332 (3)
H8A	0.3998	0.2916	0.9527	0.040*
C9	0.2468 (2)	0.5017 (2)	0.95705 (15)	0.0371 (3)
H9A	0.1618	0.4746	1.0246	0.044*
C10	0.23278 (19)	0.6499 (2)	0.89948 (15)	0.0356 (3)
H10A	0.1372	0.7262	0.9261	0.043*

C11	0.36003 (17)	0.68556 (15)	0.80251 (13)	0.0259 (3)
H11A	0.3516	0.7883	0.7655	0.031*

Atomic displacement parameters (Å²)

	U^{11}	U^{22}	U^{33}	U^{12}	U^{13}	U^{23}
Mn1	0.01447 (12)	0.00843 (11)	0.01996 (12)	−0.00059 (8)	0.00022 (9)	−0.00054 (8)
Mn2	0.01320 (9)	0.00939 (9)	0.02067 (10)	−0.00066 (6)	0.00036 (6)	−0.00119 (6)
N1	0.0203 (5)	0.0181 (5)	0.0210 (5)	−0.0024 (4)	−0.0005 (4)	−0.0009 (4)
O1	0.0210 (4)	0.0158 (4)	0.0257 (4)	0.0004 (3)	0.0040 (3)	−0.0012 (3)
O2	0.0184 (4)	0.0155 (4)	0.0233 (4)	−0.0004 (3)	0.0024 (3)	−0.0013 (3)
O3	0.0136 (4)	0.0121 (4)	0.0250 (4)	−0.0018 (3)	−0.0013 (3)	−0.0009 (3)
O4	0.0309 (5)	0.0144 (4)	0.0435 (6)	−0.0071 (4)	−0.0014 (4)	−0.0084 (4)
O5	0.0205 (4)	0.0134 (4)	0.0210 (4)	−0.0016 (3)	−0.0036 (3)	−0.0026 (3)
O6	0.0365 (6)	0.0294 (5)	0.0333 (5)	0.0076 (4)	−0.0169 (4)	−0.0090 (4)
O7	0.0199 (5)	0.0234 (5)	0.0353 (5)	0.0055 (4)	−0.0067 (4)	−0.0077 (4)
C1	0.0148 (5)	0.0180 (5)	0.0196 (5)	−0.0031 (4)	−0.0002 (4)	−0.0030 (4)
C2	0.0317 (7)	0.0305 (7)	0.0275 (7)	0.0002 (6)	0.0113 (6)	0.0015 (5)
C3	0.0173 (5)	0.0139 (5)	0.0181 (5)	−0.0030 (4)	−0.0016 (4)	−0.0023 (4)
C4	0.0151 (6)	0.0221 (6)	0.0538 (9)	−0.0011 (5)	−0.0061 (6)	−0.0023 (6)
C5	0.0206 (6)	0.0163 (5)	0.0202 (5)	−0.0039 (4)	−0.0003 (4)	−0.0018 (4)
C6	0.0425 (8)	0.0253 (7)	0.0275 (7)	0.0034 (6)	−0.0074 (6)	−0.0115 (5)
C7	0.0326 (7)	0.0196 (6)	0.0253 (6)	−0.0049 (5)	0.0002 (5)	−0.0003 (5)
C8	0.0452 (8)	0.0298 (7)	0.0267 (7)	−0.0178 (6)	−0.0018 (6)	0.0047 (5)
C9	0.0303 (7)	0.0543 (10)	0.0262 (7)	−0.0171 (7)	0.0027 (6)	0.0065 (6)
C10	0.0250 (7)	0.0472 (9)	0.0264 (7)	0.0041 (6)	0.0042 (5)	0.0007 (6)
C11	0.0248 (6)	0.0257 (6)	0.0217 (6)	0.0026 (5)	0.0000 (5)	0.0018 (5)

Geometric parameters (Å, º)

Mn1—O1	2.1369 (9)	O7—H72	0.78 (2)
Mn1—O1^{i}	2.1369 (9)	C1—C2	1.5094 (17)
Mn1—O3	2.1997 (8)	C2—H2A	0.9800
Mn1—O3^{i}	2.1997 (8)	C2—H2B	0.9800
Mn1—O5^{i}	2.2277 (8)	C2—H2C	0.9800
Mn1—O5	2.2277 (8)	C3—C4	1.4985 (17)
Mn2—O4^{ii}	2.0995 (9)	C4—H4A	0.9800
Mn2—O2	2.1579 (9)	C4—H4B	0.9800
Mn2—O7	2.1755 (10)	C4—H4C	0.9800
Mn2—O3	2.2215 (8)	C5—C6	1.5092 (17)
Mn2—O5	2.2494 (8)	C6—H6A	0.9800
Mn2—N1	2.2946 (10)	C6—H6B	0.9800
N1—C7	1.3392 (16)	C6—H6C	0.9800
N1—C11	1.3395 (16)	C7—C8	1.3819 (19)
O1—C1	1.2542 (14)	C7—H7A	0.9500
O2—C1	1.2625 (14)	C8—C9	1.376 (2)
O3—C3	1.2796 (14)	C8—H8A	0.9500
O4—C3	1.2352 (14)	C9—C10	1.383 (2)

O4—Mn2^{ii}	2.0995 (9)	C9—H9A	0.9500
O5—C5	1.2870 (15)	C10—C11	1.3833 (19)
O6—C5	1.2343 (16)	C10—H10A	0.9500
O7—H71	0.81 (2)	C11—H11A	0.9500
O1—Mn1—O1^{i}	180.0	H71—O7—H72	108 (2)
O1—Mn1—O3	86.76 (3)	O1—C1—O2	125.21 (11)
O1^{i}—Mn1—O3	93.24 (3)	O1—C1—C2	116.92 (11)
O1—Mn1—O3^{i}	93.24 (3)	O2—C1—C2	117.87 (11)
O1^{i}—Mn1—O3^{i}	86.76 (3)	C1—C2—H2A	109.5
O3—Mn1—O3^{i}	180.0	C1—C2—H2B	109.5
O1—Mn1—O5^{i}	91.39 (3)	H2A—C2—H2B	109.5
O1^{i}—Mn1—O5^{i}	88.61 (3)	C1—C2—H2C	109.5
O3—Mn1—O5^{i}	101.79 (3)	H2A—C2—H2C	109.5
O3^{i}—Mn1—O5^{i}	78.21 (3)	H2B—C2—H2C	109.5
O1—Mn1—O5	88.61 (3)	O4—C3—O3	122.80 (11)
O1^{i}—Mn1—O5	91.39 (3)	O4—C3—C4	119.24 (11)
O3—Mn1—O5	78.21 (3)	O3—C3—C4	117.94 (10)
O3^{i}—Mn1—O5	101.79 (3)	C3—C4—H4A	109.5
O5^{i}—Mn1—O5	180.0	C3—C4—H4B	109.5
O4^{ii}—Mn2—O2	88.84 (4)	H4A—C4—H4B	109.5
O4^{ii}—Mn2—O7	88.67 (4)	C3—C4—H4C	109.5
O2—Mn2—O7	95.57 (4)	H4A—C4—H4C	109.5
O4^{ii}—Mn2—O3	105.82 (4)	H4B—C4—H4C	109.5
O2—Mn2—O3	89.30 (3)	O6—C5—O5	124.09 (11)
O7—Mn2—O3	164.84 (4)	O6—C5—C6	118.89 (12)
O4^{ii}—Mn2—O5	176.87 (4)	O5—C5—C6	117.01 (11)
O2—Mn2—O5	91.19 (3)	C5—C6—H6A	109.5
O7—Mn2—O5	88.22 (4)	C5—C6—H6B	109.5
O3—Mn2—O5	77.31 (3)	H6A—C6—H6B	109.5
O4^{ii}—Mn2—N1	93.24 (4)	C5—C6—H6C	109.5
O2—Mn2—N1	173.79 (3)	H6A—C6—H6C	109.5
O7—Mn2—N1	90.33 (4)	H6B—C6—H6C	109.5
O3—Mn2—N1	84.51 (3)	N1—C7—C8	123.28 (13)
O5—Mn2—N1	87.05 (3)	N1—C7—H7A	118.4
C7—N1—C11	117.44 (11)	C8—C7—H7A	118.4
C7—N1—Mn2	119.52 (9)	C9—C8—C7	118.76 (13)
C11—N1—Mn2	122.07 (8)	C9—C8—H8A	120.6
C1—O1—Mn1	135.91 (8)	C7—C8—H8A	120.6
C1—O2—Mn2	129.37 (8)	C8—C9—C10	118.72 (13)
C3—O3—Mn1	136.43 (7)	C8—C9—H9A	120.6
C3—O3—Mn2	120.89 (7)	C10—C9—H9A	120.6
Mn1—O3—Mn2	98.99 (3)	C9—C10—C11	119.02 (14)
C3—O4—Mn2^{ii}	161.58 (10)	C9—C10—H10A	120.5
C5—O5—Mn1	135.62 (7)	C11—C10—H10A	120.5
C5—O5—Mn2	126.01 (7)	N1—C11—C10	122.75 (13)
Mn1—O5—Mn2	97.33 (3)	N1—C11—H11A	118.6
Mn2—O7—H71	107.7 (15)	C10—C11—H11A	118.6

Mn2—O7—H72	134.9 (15)		
Mn1—O1—C1—O2	−1.0 (2)	Mn2—O5—C5—O6	27.84 (17)
Mn1—O1—C1—C2	178.82 (10)	Mn1—O5—C5—C6	14.66 (17)
Mn2—O2—C1—O1	0.83 (18)	Mn2—O5—C5—C6	−150.87 (9)
Mn2—O2—C1—C2	−178.99 (9)	C11—N1—C7—C8	0.8 (2)
Mn2^{ii}—O4—C3—O3	−85.5 (3)	Mn2—N1—C7—C8	−168.22 (11)
Mn2^{ii}—O4—C3—C4	96.5 (3)	N1—C7—C8—C9	0.5 (2)
Mn1—O3—C3—O4	−177.30 (9)	C7—C8—C9—C10	−0.4 (2)
Mn2—O3—C3—O4	−24.02 (16)	C8—C9—C10—C11	−0.8 (2)
Mn1—O3—C3—C4	0.76 (18)	C7—N1—C11—C10	−2.0 (2)
Mn2—O3—C3—C4	154.04 (9)	Mn2—N1—C11—C10	166.62 (11)
Mn1—O5—C5—O6	−166.63 (10)	C9—C10—C11—N1	2.1 (2)

Symmetry codes: (i) −*x*+1, −*y*+2, −*z*+1; (ii) −*x*+1, −*y*+1, −*z*+1.

Hydrogen-bond geometry (Å, º)

D—H···*A*	*D*—H	H···*A*	*D*···*A*	*D*—H···*A*
O7—H71···O6	0.81 (2)	1.92 (2)	2.6694 (15)	154 (2)
O7—H72···O2^{iii}	0.78 (2)	2.05 (2)	2.8162 (13)	169 (2)

Symmetry code: (iii) −*x*+2, −*y*+1, −*z*+1.